

Research Article

Magnetic Fe₃O₄/Ag Hybrid Nanoparticles as Surface-Enhanced Raman Scattering Substrate for Trace Analysis of Furazolidone in Fish Feeds

Wansong Yu, Yiqun Huang, Lu Pei, Yuxia Fan, Xiaohui Wang, and Keqiang Lai

College of Food Science and Technology, Shanghai Ocean University, 999 Hucheng Huan Road, Lingang New City, Shanghai 201306, China

Correspondence should be addressed to Keqiang Lai; kqlai@shou.edu.cn

Received 7 May 2014; Revised 6 July 2014; Accepted 8 July 2014; Published 23 July 2014

Academic Editor: Bin Zhang

Copyright © 2014 Wansong Yu et al. This is an open access article distributed under the Creative Commons Attribution License, which permits unrestricted use, distribution, and reproduction in any medium, provided the original work is properly cited.

Nanoparticles (NPs) composed of ferromagnetic and noble metal materials show dual functions of magnetic activity and local surface plasmon response and have great potential as substrates for surface-enhanced Raman scattering (SERS) in trace analysis. Easy-to-prepare superparamagnetic Fe₃O₄/Ag hybrid NPs were synthesized and optimized by adjusting the ratio of silver particles aggregated with APTMS-modified Fe₃O₄ NPs. The hybrid NPs were assembled under an external magnetic field before being used as substrate for SERS analysis. The SERS spectral features of furazolidone standard solution were clearly identified at concentrations as low as 40 ng mL⁻¹, and furazolidone in fish feeds could be detected at 500 ng g⁻¹. The results indicated that the Fe₃O₄/Ag hybrid NPs as SERS substrates had a great potential for detection of trace amount of furazolidone and other prohibited or restricted antibiotics in the animal and fish feeds.

1. Introduction

Surface-enhanced Raman scattering or surface-enhanced Raman spectroscopy (SERS) has emerged as an important tool for trace analysis in many fields, such as chemistry, biology, environment, and food due to its ultrahigh sensitivity and potential rapidity or nondestructivity [1–3]. Raman enhancement effect is mainly attributed to the surface plasmon resonance (SPR) very close to the surface of nanostructured noble metal substrate [4, 5]. Enormous SPR is often present at the gaps between microstructures, resulting in the so-called hot spots. In general, nanoparticles suspended in a well-dispersed system containing target molecules lead to rather weak SERS signals, while aggregated NPs result in better enhancement effect since more interparticle narrow gaps could be provided on the surface of aggregated colloids [6]. The use of magnetic oxides/noble metal hybrid NPs makes it possible to assemble NPs in a relative orderly aggregated pattern with the assistance of an external magnetic field and has shown great advantages as SERS substrates [7–9]. For instance, Hu and Sun reported a robust strategy

to construct Au coated multilayer magnetic nanoparticles with tunable hot spots by controlling the seed-mediated plating process, resulting in ultrasensitive SERS detection for rhodamine 6G as low as femtomolar [7]. Bao et al. fabricated Ag-Fe₃O₄ NPs and maximized SERS sensitivity through changing the size and density of Ag particles. The optimized NPs could be used to detect rhodamine 6G at a concentration as low as 10⁻¹² [8]. Wheeler et al. demonstrated that magnetically induced aggregation of the Fe₃O₄-Au core-shell NPs enhanced SERS activity for ~7 times compared to nonmagnetically aggregated Fe₃O₄-Au NPs [9].

SERS is considered as first layer effect, and the analyte molecules must be very close to or adsorbed onto substrates to achieve significant enhancement effect. The surface of a SERS substrate must be clean so that targeted molecules could be adsorbed onto the surface. However, precursors and reducing agents used during NPs synthesis are often present on the surface of NPs, interfering with effective adsorption of analytes molecules [10]. The precursors and reducing agents used for the synthesis of noble metal-coated Fe₃O₄ NPs could be washed off under an externally exerted magnetic force,

resulting in clean substrate surfaces. Therefore, magnetic noble metal NPs often lead to higher enhancement effects than nonmagnetic NPs [11].

The objective of this study was to synthesize $\text{Fe}_3\text{O}_4/\text{Ag}$ hybrid NPs suitable for analysis of trace amounts of furazolidone in animal feeds. Furazolidone is a nitrofurantoin antibiotic often applied illegally as animal or fish feeds, although it is prohibited by many countries due to its carcinogenicity and other adverse health effects [12]. There are very few studies published on the application of SERS for analysis of nitrofurantoin antibiotics, and these studies mainly used standard solutions instead of actual samples [13–15]. To the best of our knowledge, there is no report on applying SERS to analyze nitrofurantoin antibiotics in animal or fish feeds. Complex sample systems (such as fish feeds) contain numerous nontargeted compounds that may interfere with and sometimes even make it impossible for the SERS analysis of targeted molecules. In this study, easy-to-prepare superparamagnetic $\text{Fe}_3\text{O}_4/\text{Ag}$ hybrid NPs were synthesized and applied for trace detection of furazolidone in fish feeds with pronounced SERS activity, which helps understand the matrix effects on the SERS analysis and serves as a basis for further studies on rapid SERS method development for nitrofurantoin antibiotics in complex animal/fish feed systems.

2. Materials and Methods

2.1. Reagents. Analytical grade ferric chloride ($\text{FeCl}_3 \cdot 6\text{H}_2\text{O}$), ferrous chloride ($\text{FeCl}_2 \cdot 4\text{H}_2\text{O}$), ethanol, sodium hydroxide, ammonia solution (30%), dichloromethane, anhydrous sodium sulfate, alumina, acetonitrile (HPLC grade), and hexane (HPLC grade) were purchased from Sinopharm Chemical Reagent Co., Ltd. (number 52 Ningbo Road, Shanghai, China); silver nitrate ($\geq 99\%$), hydroxylamine hydrochloride ($\geq 99\%$), 3-aminopropyltrimethoxysilane (APTMS, 97%), and furazolidone (ACS grade) were obtained from Sigma-Aldrich (St. Louis, MO, USA). All aqueous solutions were prepared using ultrapure water ($18.2 \text{ M}\Omega \text{ cm}$).

2.2. Synthesis of $\text{Fe}_3\text{O}_4/\text{Ag}$ Hybrid NPs. The coprecipitation method was used to synthesize Fe_3O_4 NPs, in which ferric and ferrous ions (molar ratio 2:1) were coprecipitated to Fe_3O_4 in alkaline solutions at room temperature and the resultants were treated under hydrothermal conditions [16, 17]. The as-synthesized iron oxide particles were hydrophilic, which could be easily dispersed in AgNO_3 solutions for later Ag particles growing and aggregating with Fe_3O_4 NPs. The reaction was performed under oxygen-free environment by passing N_2 gas. In brief, $\text{FeCl}_3 \cdot 6\text{H}_2\text{O}$ (5.40 g) and $\text{FeCl}_2 \cdot 4\text{H}_2\text{O}$ (1.99 g) were thoroughly mixed in 100 mL water. Next, $\text{NH}_3 \cdot \text{H}_2\text{O}$ (30%) was added with vigorous stirring until the pH was 10, and the mixture was continuously stirred for 10 minutes at room temperature. The mixture was then heated at 80°C for 30 min. Following this, the mixture was washed under magnetic field with ethanol and water three times for each and then dried in vacuum oven at 70°C for 2 hours.

To be able to attach Ag particles and Fe_3O_4 NPs, APTMS was used as a linker between Fe_3O_4 and Ag NPs [18, 19].

To obtain APTMS-modified Fe_3O_4 NPs, Fe_3O_4 NPs (0.25 g) were added into ethanol (100 mL) and sonicated for 40 minutes. Next, APTMS (1 mL) was added to the mixture followed by stirring for 6 hours. Then the mixture was rinsed four times with ethanol under an external magnetic field and dried in a vacuum oven at 70°C for 2 hours.

Four different types of hybrid NPs were constructed by aggregation of APTMS-modified Fe_3O_4 NPs and Ag particles through adjusting the molar ratio of AgNO_3 and Fe_3O_4 NPs (2:1, 3:1, 4:1, 5:1). The amount of Fe_3O_4 NPs was fixed (0.05 g, 0.22 mmol), and four different levels of AgNO_3 solutions (0.07 g, 0.44 mmol; 0.11 g, 0.66 mmol; 0.15 g, 0.88 mmol; 0.19 g, 1.10 mmol) were mixed with Fe_3O_4 NPs and sonicated for 40 minutes, respectively. Then, freshly prepared reductant mixtures consisting of 50 mL 0.1 M NaOH and 45 mL 0.06 M hydroxylamine hydrochloride were added dropwise and mixed for 45 minutes. Finally, the NPs were washed with water under an external magnetic field until the supernatant was clear. The four $\text{Fe}_3\text{O}_4/\text{Ag}$ hybrid NPs samples were labeled as FA-1, FA-2, FA-3, and FA-4, respectively. Figure 1 is a summary of the procedure for synthesis of $\text{Fe}_3\text{O}_4/\text{Ag}$ hybrid NPs and later substrate preparation.

2.3. Characterization of Composite Nanoparticles. General shapes and sizes of Fe_3O_4 NPs and $\text{Fe}_3\text{O}_4/\text{Ag}$ hybrid NPs were characterized by a JEM-2100F transmission electron microscopy (TEM; JEOL Ltd., Tokyo, Japan). The samples for TEM characteristics were prepared by making a carbon-coated copper grid soaked in as-prepared NPs for 30 minutes before being dried at room temperature. Scanning TEM equipped with a high angle annular dark field detector (STEM-HAADF) and energy dispersive spectroscopy (EDS) elemental mapping was used to further understand the structure and component of particles. The magnetic properties were investigated by using a Quantum Design superconducting quantum interference device (SQUID) magnetometer (MPMS SQUID VSM, Quantum Design Ltd., USA) at room temperature.

2.4. Preparation of Fish Feed Samples. Fish feeds from the College of Fisheries and Life Science in Shanghai Ocean University were spiked with furazolidone at a series of concentrations (200, 500, 1000, and 5000 ng mL^{-1}). Furazolidone was then extracted and purified from fish feeds based upon the method of Hu et al. [20]. In brief, furazolidone was extracted with dichloromethane three times and purified through anhydrous sodium sulfate and alumina column successively. The column was a syringe (10 mL) containing a filtration membrane ($0.45 \mu\text{m}$), 4.0 g of anhydrous sodium sulfate, and 2.0 g of alumina. The eluate was evaporated to almost dryness at 50°C in water base with a rotary evaporator (R206B, Shanghai SENCO Technology Ltd., Shanghai, China), dissolved into 1.0 mL of acetonitrile/water (8:2) and 1.0 mL of hexane, and then centrifuged. The supernatant hexane was discarded, followed by adding 1.0 mL of hexane to defat the matrix. Finally, the supernatant was collected and used for SERS analysis.

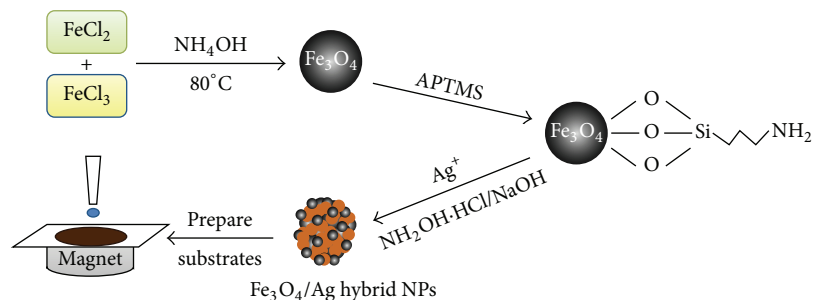


FIGURE 1: Schematic illustration of major steps for synthesis of Fe₃O₄/Ag hybrid NPs and preparation of SERS substrates.

2.5. SERS Analysis. A series of furazolidone standard solutions (1000, 500, 100, 50, 40, and 20 ng mL⁻¹) were prepared in acetonitrile. For SERS measurement, 10 μL of Fe₃O₄/Ag NPs was first added onto a glass slide on top of the magnet, and furazolidone standard solution was added on top of NPs droplets. After the substrates were dried under ambient conditions, 20 spectra were collected at different positions of the substrates and the average of these spectra was used as the final spectrum for the sample. To compare the enhancement effect of four different Fe₃O₄/Ag hybrid NPs, SERS spectra of furazolidone standards (100 and 500 ng mL⁻¹) were collected with each type of NPs, respectively, and the experiments were repeated five times. In addition, SERS enhancement effect without the use of magnetic field was examined by removing the magnetic field during Fe₃O₄/Ag NPs substrate preparation for the SERS measurement.

The SERS measurement of Fe₃O₄/Ag NPs with different amounts of silver was carried out on a Nicolet DXR microscopy Raman spectrometer (Thermo Fisher Scientific Inc., Waltham, MA, USA). A 780 nm HP He-Ne laser source with 20 mW laser power and a 20x objective was used for spectral collection. All spectra were recorded with a 2-second exposure time for each scan, and the final spectra were the sum of two scans.

3. Results and Discussion

3.1. Characterization of Fe₃O₄/Ag Hybrid NPs. The TEM images of Fe₃O₄ NPs are exhibited in Figure 2(a), and their average diameter was 12 ± 1 nm calculated from 100 particles. The Fe₃O₄ NPs had relative uniform and narrow size distribution (standard deviation 9% < 10% [21]). Figure 2(b) shows TEM images of representative Fe₃O₄/Ag hybrid NPs (FA-3) synthesized in this study, in which the lighter small particles are Fe₃O₄, while the darker large particles are Fe₃O₄/Ag hybrid NPs (FA-3). The figure indicates that APTMS-modified Fe₃O₄ NPs are successfully aggregated with Ag particles. Through the condensation reaction between -OH groups on the surface of Fe₃O₄ NPs and APTMS, NH₂ groups are then decorated on the Fe₃O₄ NPs, which allows for coordination and static binding of Ag particles with negatively charged surface [18]. Figure 2(c) shows statistical histogram of diameters and relative standard deviation (RSD) of four Fe₃O₄/Ag hybrid NPs (*n* = 100). The particle sizes were 58 ± 7 nm, 63 ± 8 nm, 73 ± 9 nm,

and 106 ± 14 nm, respectively, increasing gradually with an increase of molar concentration of Ag⁺ ions used for hybrid NPs aggregation. The size distributions of four samples were all less than 15%, indicating relatively uniform particle size. Figure 2(d) is the EDS spectrum of Fe₃O₄/Ag NPs, which shows the peaks corresponding to Ag and Fe elements. The presence of Cu elements was due to the carbon-coated copper grid used as the holder for nanoparticles. The STEM-HAADF image and element mapping images for Fe₃O₄/Ag NPs indicate that Fe₃O₄/Ag hybrid NPs are aggregates of Fe₃O₄ and Ag particles and contain denser Ag particles than Fe₃O₄ particles (Figures 3(a)–3(d)).

Figure 4 exhibits the magnetization curves of dried Fe₃O₄ NPs and two Fe₃O₄/Ag hybrid NPs (FA-3 and FA-4) measured at room temperature. The saturated magnetization (SM) value of Fe₃O₄ NPs was 83.0 emu·g⁻¹, which was higher than 78.0 emu·g⁻¹ reported by Kim et al. [22] and 53.7 emu·g⁻¹ by Bao et al. [8]. The negligible coercivity and reversible hysteresis behavior indicated the superparamagnetic nature of Fe₃O₄ NPs, which is common for magnetite smaller than 30 nm in diameter [23]. The SM values of FA-3 and FA-4 were 46.7, 36.5 emu·g⁻¹, respectively. The SM values decreased with an increase of Ag ratio in the hybrid NPs due to the diamagnetic contribution of Ag particles [22]. The magnetic response for all four hybrid NPs is strong enough to make it easy to rinse the NPs and to conduct magnetically induced aggregation in a magnetic field. The excellent magnetic property of hybrid NPs also allows separating the particles over a short time (less than 30 seconds) in an external magnetic field (Figures 4(D) and 4(E)).

3.2. Effect of Magnetic Self-Assembly Method on SERS Sensitivity. In order to understand the effect of the ratio of Ag particles on the SERS sensitivity, four different Fe₃O₄/Ag hybrid NPs were used as substrates to collect the SERS spectra of furazolidone standards 100 and 500 ng mL⁻¹, respectively. Figure 5(a) displayed the representative SERS spectra of 500 ng mL⁻¹ furazolidone acquired with the use of four hybrid NPs substrates. All four spectra consist of characteristic peaks at 1561, 1490, 1348, and 1014 cm⁻¹ associated with furan ring stretching vibrations. The peak at 1606 cm⁻¹ is assigned to C=N stretching vibration in the plane, while medium bands at 1243, 960, and 807 cm⁻¹ are attributed to

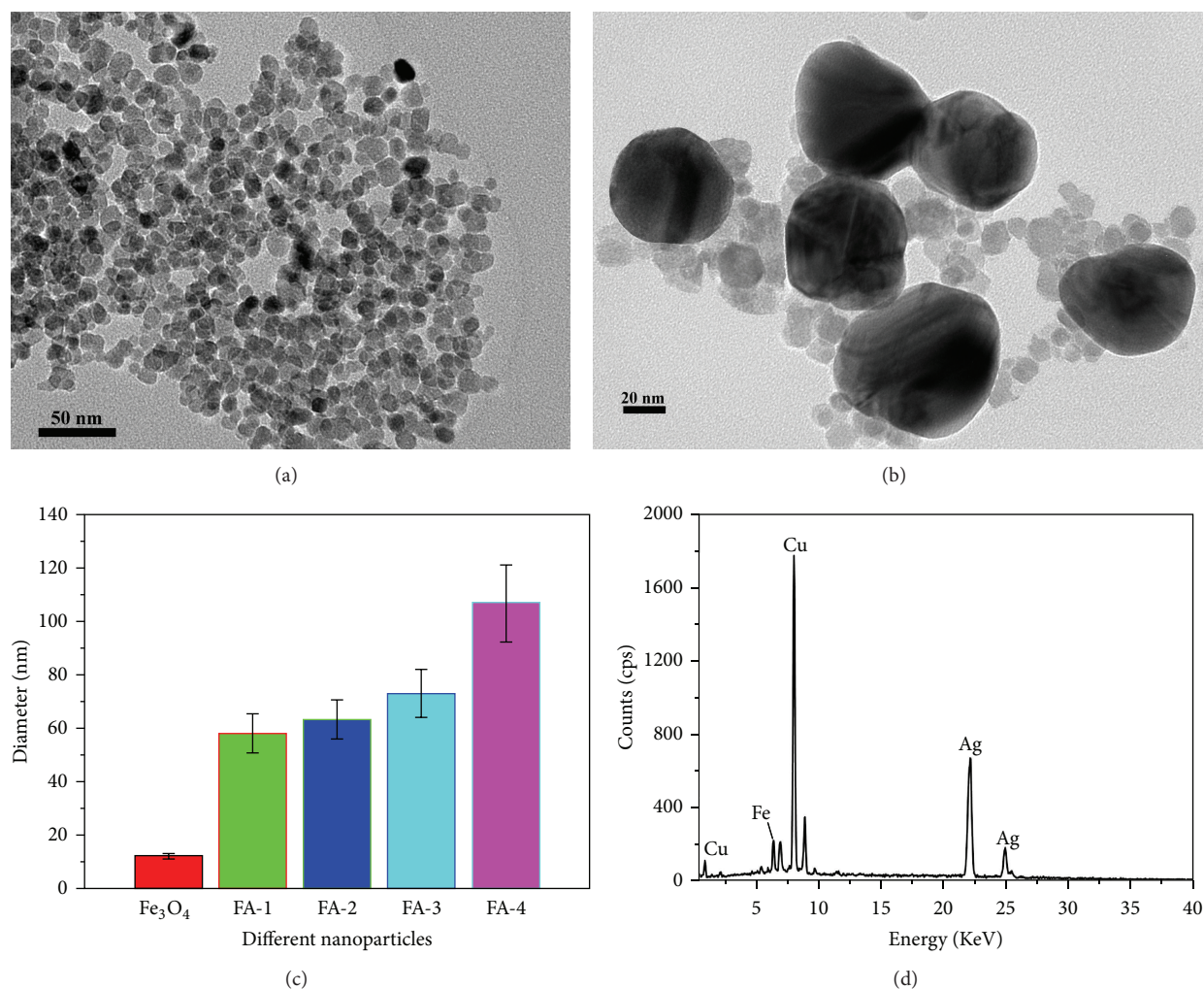


FIGURE 2: TEM images of (a) Fe₃O₄ NPs and (b) Fe₃O₄/Ag hybrid NPs (FA-3) at a 4 : 1 molar ratio of Ag⁺ and Fe₃O₄; (c) statistical histogram of diameters of four types of Fe₃O₄/Ag hybrid NPs ($n = 100$) and (d) EDS spectrum of representative Fe₃O₄/Ag hybrid NPs.

C–H bending vibrations and C–C stretching vibrations [13]. Notably, the SERS signals from FA-3 were much stronger than the others. Similar trends were observed for SERS spectra of 100 ng mL⁻¹ furazolidone. Using the characteristic peak at 1348 cm⁻¹ as an example (Figure 5(b)), its Raman intensity increased with an increase in hybrid particle size until reaching 73 ± 9 nm but then decreased with a further increase of particle size. Controlling the amount of Ag particles aggregated with modified-Fe₃O₄ NPs through adjusting the molar ratio of Ag⁺ ions and Fe₃O₄ NPs makes the SPR tunable and eventually optimizes Raman enhancement effect for furazolidone. In addition, although it is often a challenge to obtain reproducible SERS spectra, by using the average of spectra collected at 20 different positions of a substrate, we can overcome this problem. As shown in Figure 5(b) for the Raman intensity of 500 ng mL⁻¹ and 100 ng mL⁻¹, with furazolidone at the characteristic peak of 1348 cm⁻¹, the error bars calculated from quintuplicate analyses indicated very small standard deviation for spectra collected independently,

implying that repeatable spectra could be obtained with Fe₃O₄/Ag hybrid NPs.

We also attempted to analyze furazolidone with Ag NPs varying in particle size (34–67 nm) synthesized using the method of Leopold and Lendl [24], but very weak SERS enhancement was obtained. This was probably due to the interference of remaining reductive agent on the surface of Ag NPs that affected the effective adsorption of furazolidone. On the contrary, the surface of Fe₃O₄/Ag hybrid NPs was clean because reductive agent and other nontargeted compounds could be removed by washing with copious amounts of water under external magnetic field before the NPs were used for SERS analysis.

Using a magnetically directed self-assembly method is a simple and effective way to condense NPs on a glass slide used as holder for substrate and analyte molecules to increase SERS signals [6]. Figure 6 shows the SERS spectra of furazolidone obtained using 73 ± 9 nm Fe₃O₄/Ag hybrid NPs assembled onto a glass slide with and without an external magnetic field.

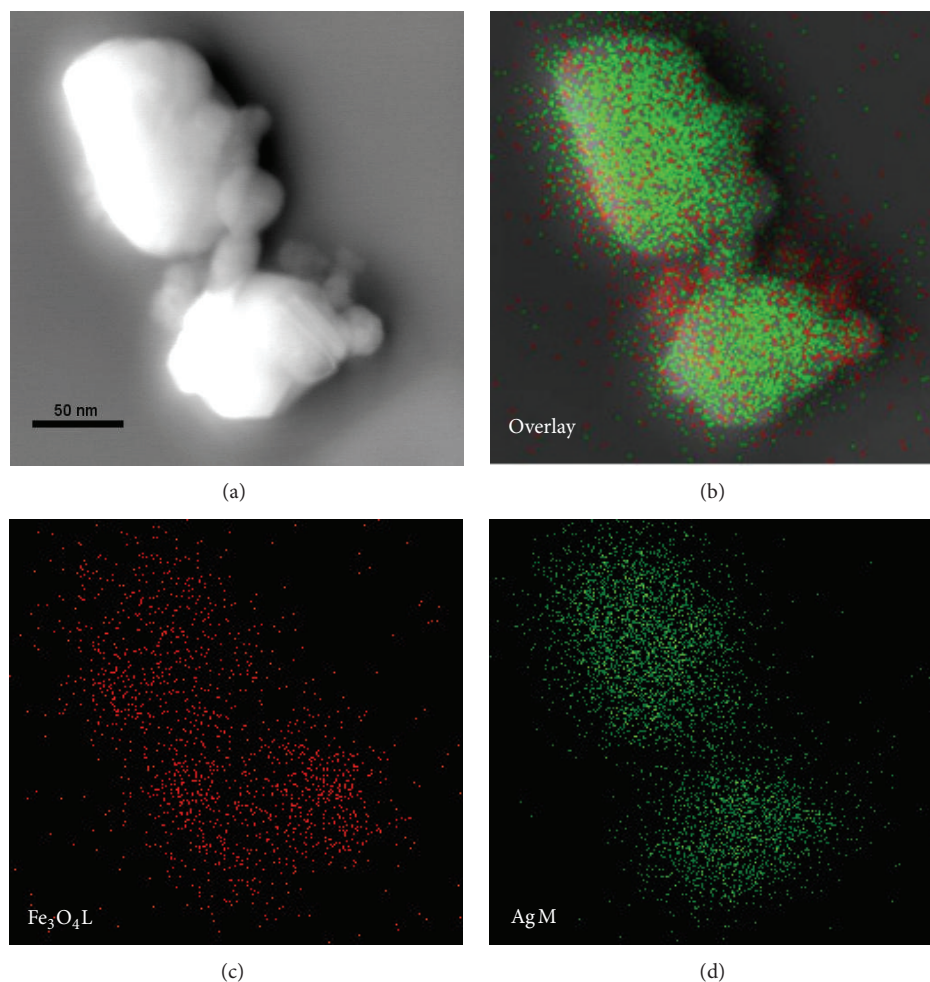


FIGURE 3: (a) STEM-HAADF images of $\text{Fe}_3\text{O}_4/\text{Ag}$ hybrid NPs (FA-3); (b)–(d) EDS elemental mapping images of FA-3: (b) overlay, (c) Fe_3O_4 L map, and (d) Ag M map.

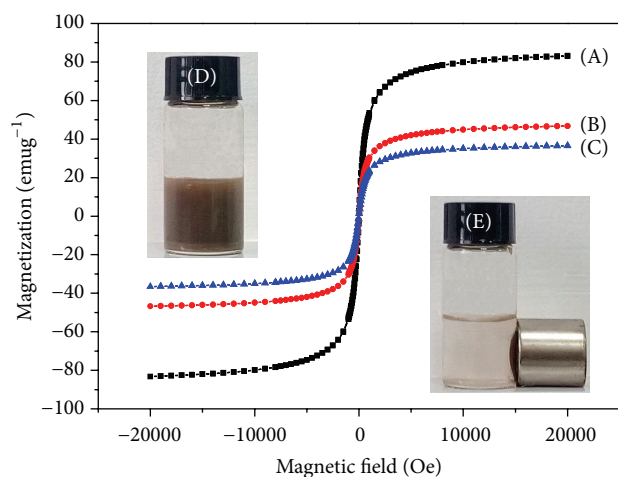


FIGURE 4: Magnetization curves of (A) Fe_3O_4 NPs, (B) $\text{Fe}_3\text{O}_4/\text{Ag}$ hybrid NPs (FA-3), and (C) $\text{Fe}_3\text{O}_4/\text{Ag}$ hybrid NPs (FA-4); (D) the sample of FA-3 and (E) separation of FA-3 by an external magnetic field.

The spectra obtained with substrates assembled under magnetic field displayed stronger SERS signals, with about twice to fourfold increase in enhancement effect compared to those without magnetic field. NPs assembled in a more orderly arrangement by the magnetic force led to the formation of more relatively homogeneous SERS hot spots and therefore better enhancement effect [6].

The FA-3 $\text{Fe}_3\text{O}_4/\text{Ag}$ hybrid NPs were used as SERS substrate to further acquire spectra of furazolidone with different concentrations, as shown in Figure 7(a), characteristic peaks of furazolidone were clearly visible at concentration as low as 40 ng mL^{-1} , and the intensity of SERS signals increased as the concentration changed from 40 to 1000 ng mL^{-1} . This indicated that $\text{Fe}_3\text{O}_4/\text{Ag}$ hybrid NPs exhibited significant Raman enhancement effect as SERS substrate for furazolidone detection.

3.3. SERS Analysis of Furazolidone in Spiked Fish Feed Samples. The SERS-optimized spectra (acquired with FA-3

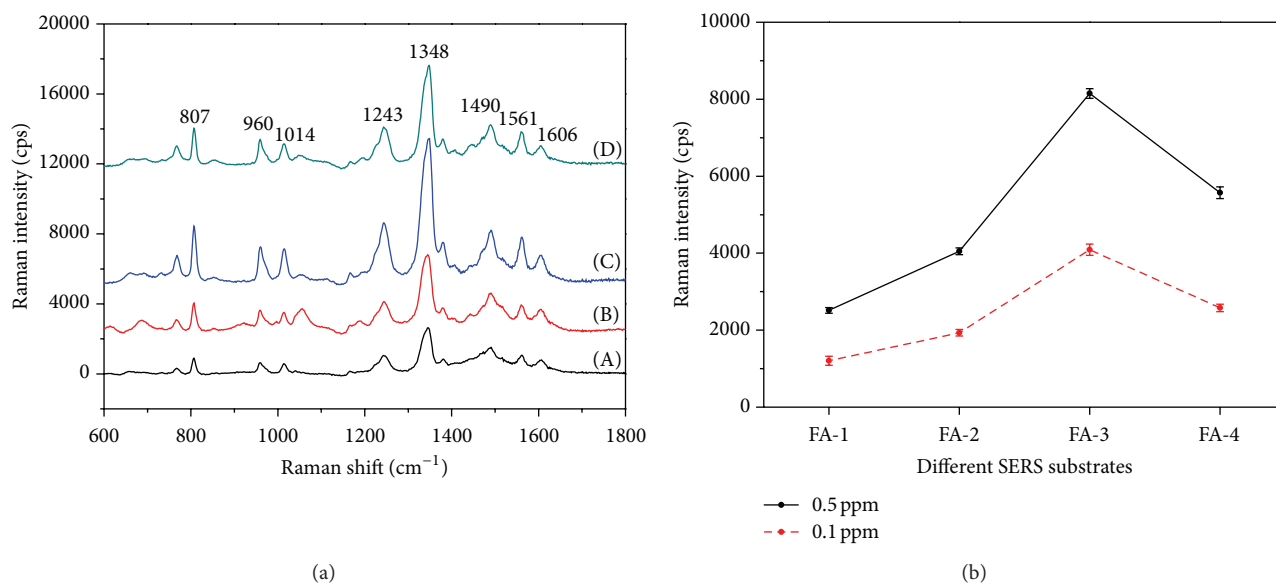


FIGURE 5: (a) Representative SERS spectra of 500 ng mL^{-1} furazolidone molecules adsorbed on (A) FA-1, (B) FA-2, (C) FA-3, and (D) FA-4; (b) Raman intensity of 500 ng mL^{-1} and 100 ng mL^{-1} furazolidone at 1348 cm^{-1} ($n = 5$).

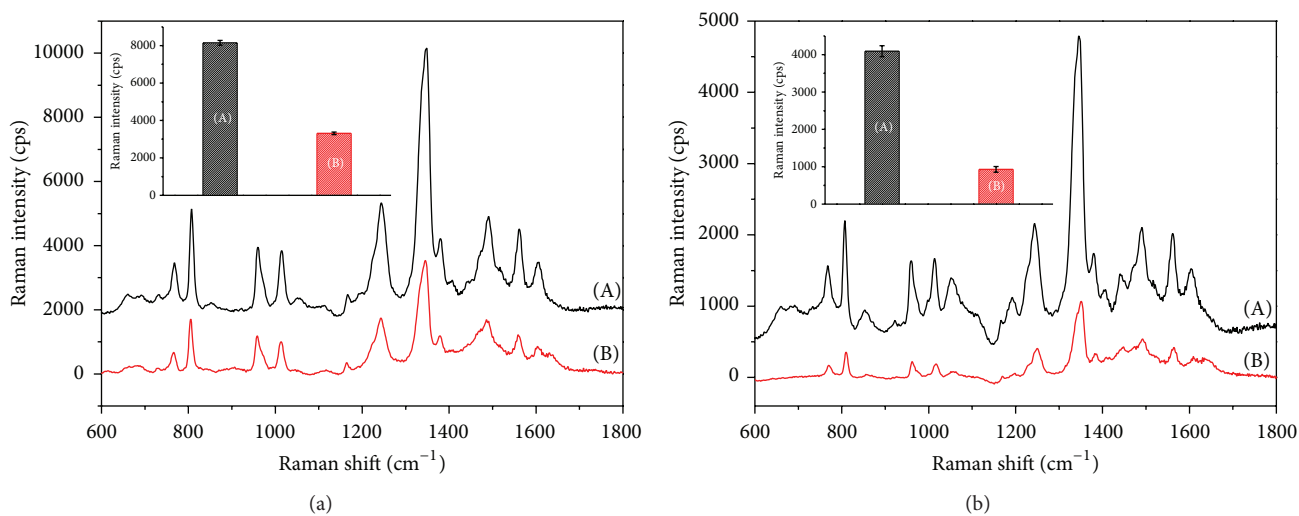


FIGURE 6: SERS spectra of (a) 500 ng mL^{-1} and (b) 100 ng mL^{-1} furazolidone molecules adsorbed on the FA-3 substrates prepared by magnetically directed self-assembly method (curve A) and nonmagnetic force (curve B). (The inset was the mean Raman intensity at 1348 cm^{-1} corresponding to curves A and B.)

hybrid NPs) of extracts from spiked fish feeds consist of main characteristic peaks of furazolidone consistent with those of the standards, although some extra bands (such as the ones at around 1050 and 1447 cm^{-1}) are observed in the spectra of extracts (Figure 7(b)). These extra bands may be due to some residual compounds, such as amino acids and pigments naturally present in fish feeds. Due to the high sensitivity of SERS method, some trace amounts of nontargeted compounds from fish feed may produce SERS signals. In addition, nontargeted compounds in the extracts may interfere with effective adsorption of furazolidone molecules onto the

NPs and reduce the sensitivity of SERS method. As shown in Figure 7(b), the intensity of furazolidone characteristic peaks for extracts was weaker than that for standards. The lowest concentration with discernible characteristic peaks of furazolidone was 500 ng g^{-1} for extracts, which is much higher than that of 40 ng mL^{-1} for standards. However, the sensitivity of the SERS method for furazolidone in fish feed is comparable to a reported HPLC-UV method (detection limit, $1 \mu\text{g g}^{-1}$) [25] and a LC-MS method for animal feeds (detection limit, 100 ng g^{-1}) [26]. In addition, the sensitivity of the SERS method could meet the requirement for analysis

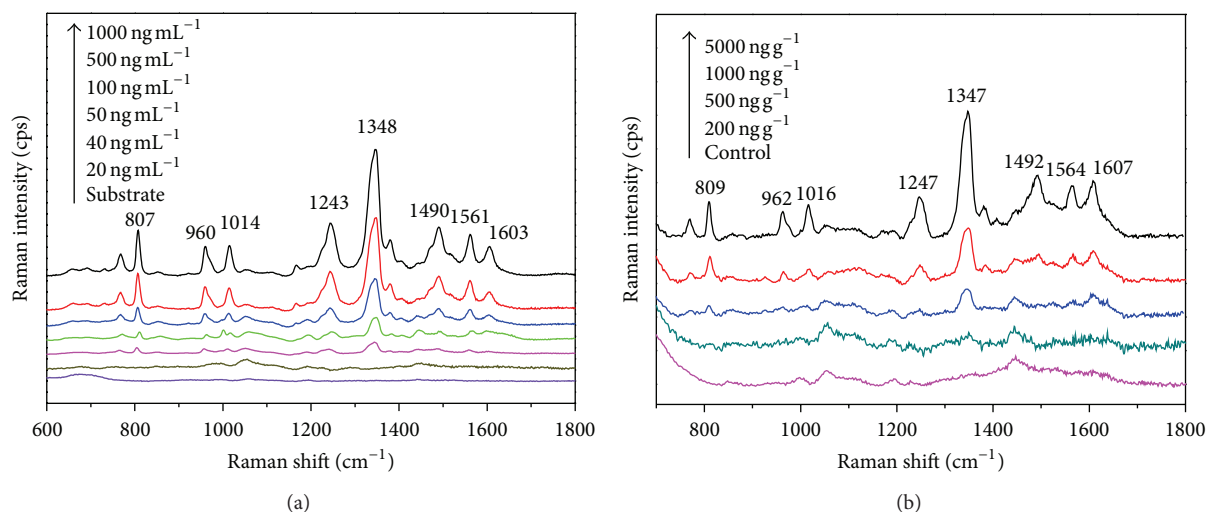


FIGURE 7: Respective SERS spectra collected with FA-3 NPs of (a) furazolidone standard solution and (b) furazolidone extracts from fish feeds.

of furazolidone in animal and fish feeds, which are often added with the antibiotics ranging from $8 \mu\text{g g}^{-1}$ to $400 \mu\text{g g}^{-1}$ [27].

4. Conclusions

Superparamagnetic Fe_3O_4 NPs were synthesized and modified using APTMS to add NH_2 groups on their surfaces and then aggregated with Ag particles to form $\text{Fe}_3\text{O}_4/\text{Ag}$ hybrid NPs. The $\text{Fe}_3\text{O}_4/\text{Ag}$ hybrid NPs exhibited tunable plasmonic properties of SERS by adjusting the amount of Ag particles aggregated with Fe_3O_4 NPs through modulating molar ratios of the Ag^+ and Fe_3O_4 . The use of $73 \pm 9 \text{ nm}$ $\text{Fe}_3\text{O}_4/\text{Ag}$ hybrid NPs assembled onto a glass slide under an external magnetic field as SERS substrate could detect furazolidone standards and furazolidone in fish feeds at the levels as low as 40 ng mL^{-1} and 500 ng g^{-1} , respectively. To improve the applicability of the SERS analysis method, simplifying sample preparation and development of selective SERS substrates are much needed for future research.

Conflict of Interests

The authors declare that there is no conflict of interests regarding the publication of this paper.

Acknowledgments

This research was supported by Innovation Program of Shanghai Municipal Education Commission (14YZ123), funding program for outstanding dissertations (B1-9600-12-0001-5), and the National Natural Science Foundation of China (61250002 and 31250006).

References

- [1] L. Pei, Y. Huang, C. Li, Y. Zhang, B. A. Rasco, and K. Lai, "Detection of triphenylmethane drugs in fish muscle by surface-enhanced Raman spectroscopy coupled with Au-Ag core-shell nanoparticles," *Journal of Nanomaterials*, vol. 2014, Article ID 730915, 8 pages, 2014.
- [2] Y. Pan, K. Q. Lai, Y. X. Fan et al., "Determination of tert-butylhydroquinone in vegetable oils using surface-enhanced Raman spectroscopy," *Journal of Food Science*, vol. 79, no. 6, pp. 1225–1230, 2014.
- [3] Y. X. Fan, K. Q. Lai, B. A. Rasco, and Y. Q. Huang, "Analyses of phosmet residues in apples with surface-enhanced Raman spectroscopy," *Food Control*, vol. 37, pp. 153–157, 2014.
- [4] B. Han, N. Choi, K. H. Kim, D. W. Lim, and J. Choo, "Application of Silver-coated magnetic microspheres to a SERS-based optofluidic sensor," *Journal of Physical Chemistry C*, vol. 115, no. 14, pp. 6290–6296, 2011.
- [5] Z. C. Xu, Y. L. Hou, and S. H. Sun, "Magnetic core/shell $\text{Fe}_3\text{O}_4/\text{Au}$ and $\text{Fe}_3\text{O}_4/\text{Au}/\text{Ag}$ nanoparticles with tunable plasmonic properties," *Journal of the American Chemical Society*, vol. 129, no. 28, pp. 8698–8699, 2007.
- [6] L. Zhang, W. Dong, Z. Tang, J. Song, H. Xia, and H. Sun, "Surface-enhanced Raman scattering substrates of high-density and high-homogeneity hot spots by magneto-metal nanoprobe assembling," *Optics Letters*, vol. 35, no. 19, pp. 3297–3299, 2010.
- [7] Y. Hu and Y. Sun, "Stable magnetic hot spots for simultaneous concentration and ultrasensitive surface-enhanced Raman scattering detection of solution analytes," *Journal of Physical Chemistry C*, vol. 116, no. 24, pp. 13329–13335, 2012.
- [8] Z. Y. Bao, J. Dai, D. Y. Lei, and Y. Wu, "Maximizing surface-enhanced Raman scattering sensitivity of surfactant-free Ag- Fe_3O_4 nanocomposites through optimization of silver nanoparticle density and magnetic self-assembly," *Journal of Applied Physics*, vol. 114, no. 12, Article ID 124305, 7 pages, 2013.
- [9] D. A. Wheeler, S. A. Adams, T. López-Luke, A. Torres-Castro, and J. Z. Zhang, "Magnetic Fe_3O_4 -Au core-shell nanostructures

- for surface enhanced Raman scattering," *Annalen der Physik*, vol. 524, no. 11, pp. 670–679, 2012.
- [10] R. A. Alvarez-Puebla and L. M. Liz-Marzán, "Traps and cages for universal SERS detection," *Chemical Society Reviews*, vol. 41, no. 1, pp. 43–51, 2012.
- [11] L. Yang, Z. Bao, Y. Wu, and J. Liu, "Clean and reproducible SERS substrates for high sensitive detection by solid phase synthesis and fabrication of Ag-coated Fe₃O₄ microspheres," *Journal of Raman Spectroscopy*, vol. 43, no. 7, pp. 848–856, 2012.
- [12] M. Nora, N. M. Angelini, O. D. Rampini, and H. Mugica, "Liquid chromatographic determination of nitrofurans residues in bovine muscle tissues," *Journal of AOAC International*, vol. 80, no. 3, pp. 481–485, 1997.
- [13] D. L. Lu, H. Y. Han, and J. Liang, "Highly sensitive silver mirror substrate preparation and its application to surface enhanced Raman spectroscopic detection of furazolidone," *Chinese Journal of Analytical Chemistry*, vol. 38, no. 5, pp. 715–718, 2010.
- [14] Y. Xie, X. Zhu, Y. Sun, H. Wang, H. Qian, and W. Yao, "Rapid detection method for nitrofurans antibiotic residues by surface-enhanced Raman Spectroscopy," *European Food Research and Technology*, vol. 235, no. 3, pp. 555–561, 2012.
- [15] Y. Y. Zhang, Y. Q. Huang, F. L. Zhai, R. Du, Y. D. Liu, and K. Q. Lai, "Analyses of enrofloxacin, furazolidone and malachite green in fish products with surface-enhanced Raman spectroscopy," *Food Chemistry*, vol. 135, no. 2, pp. 845–850, 2012.
- [16] R. V. Mehta, R. V. Upadhyay, S. W. Charles, and C. N. Ramchand, "Direct binding of protein to magnetic particles," *Biotechnology Techniques*, vol. 11, no. 7, pp. 493–496, 1997.
- [17] M. Liao and D. Chen, "Preparation and characterization of a novel magnetic nano-adsorbent," *Journal of Materials Chemistry*, vol. 12, no. 12, pp. 3654–3659, 2002.
- [18] S. Guo, S. Dong, and E. Wang, "A general route to construct diverse multifunctional Fe₃O₄ metal hybrid nanostructures," *Chemistry: A European Journal*, vol. 15, no. 10, pp. 2416–2424, 2009.
- [19] J. Du and C. Jing, "Preparation of Fe₃O₄@Ag SERS substrate and its application in environmental Cr(VI) analysis," *Journal of Colloid and Interface Science*, vol. 358, no. 1, pp. 54–61, 2011.
- [20] X. Hu, Y. Xu, and A. Yediler, "Determinations of residual furazolidone and its metabolite, 3-amino-2-oxazolidinone (AOZ), in fish feeds by HPLC-UV and LC-MS/MS, respectively," *Journal of Agricultural and Food Chemistry*, vol. 55, no. 4, pp. 1144–1149, 2007.
- [21] X. Liu, H. Xu, H. Xia, and D. Wang, "Rapid seeded growth of monodisperse, quasi-spherical, citrate-stabilized gold nanoparticles via H₂O₂ reduction," *Langmuir*, vol. 28, no. 38, pp. 13720–13726, 2012.
- [22] K. Kim, J. Choi, H. B. Lee, and K. S. Shin, "Silanization of Ag-deposited magnetite particles: an efficient route to fabricate magnetic nanoparticle-based Raman barcode materials," *ACS Applied Materials and Interfaces*, vol. 2, no. 7, pp. 1872–1878, 2010.
- [23] S. C. Hsiao, J. L. Ou, Y. Sung, C. P. Chang, and M. D. Ger, "Preparation of sulfate- and carboxyl-functionalized magnetite/polystyrene spheres for further deposition of gold nanoparticles," *Colloid and Polymer Science*, vol. 288, no. 7, pp. 787–794, 2010.
- [24] N. Leopold and B. Lendl, "A new method for fast preparation of highly surface-enhanced Raman scattering (SERS) active silver colloids at room temperature by reduction of silver nitrate with hydroxylamine hydrochloride," *The Journal of Physical Chemistry B*, vol. 107, no. 24, pp. 5723–5727, 2003.
- [25] R. J. McCracken and D. G. Kennedy, "Determination of furazolidone in animal feeds using liquid chromatography with UV and thermospray mass spectrometric detection," *Journal of Chromatography A*, vol. 771, no. 1-2, pp. 349–354, 1997.
- [26] J. R. Wang and L. Y. Zhang, "Simultaneous determination and identification of furazolidone, furaltadone, nitrofurazone, and nitrovin in feeds by HPLC and LC-MS," *Journal of Liquid Chromatography and Related Technologies*, vol. 29, no. 3, pp. 377–390, 2006.
- [27] J. Barbosa, S. Moura, R. Barbosa, F. Ramos, and M. I. N. D. Silveira, "Determination of nitrofurans in animal feeds by liquid chromatography-UV photodiode array detection and liquid chromatography-ionspray tandem mass spectrometry," *Analytica Chimica Acta*, vol. 586, no. 1-2, pp. 359–365, 2007.



Hindawi

Submit your manuscripts at
<http://www.hindawi.com>

